Original Articles

Definition criteria determine the success of old-growth mapping

Jamis M. Bruening [a,*], Ralph O. Dubayah [a], Neil Pederson [b], Benjamin Poulter [c], Leonardo Calle [c,d]

[a] *Department of Geographical Sciences, University of Maryland, College Park, MD, USA*
[b] *Harvard Forest, Harvard University, Petersham, MA, USA*
[c] *NASA Goddard Space Flight Center, Biospheric Sciences Laboratory, Greenbelt, MD, USA*
[d] *Earth System Science Interdisciplinary Center, University of Maryland, College Park, MD, USA*

ARTICLE INFO

ABSTRACT

Old-growth forests have been widely studied for decades. The extreme diversity of old forest characteristics has inspired an equally diverse set of old-growth definitions, and makes mapping old-growth difficult across large areas and different forest types. While the use of remote sensing in old-growth research is not new, there is a growing need for large scale mapping to improve understanding of old forest processes and to support old-growth conservation. Old-growth mapping requires definitions that are ecologically relevant to old forests while also transferable to remote sensing data. In this paper we develop a conceptual framework to evaluate three dimensions of old-growth—a temporal dimension related to tree ages, a physical dimension related to tree sizes, and a functional dimension related to forest processes. In the first part of our analysis, we classify forests throughout the eastern US as old or not with respect to each old-growth dimension using existing old-growth definitions and data from the US Forest Inventory and Analysis (FIA) program. We estimate the proportion of forest classified as old within a hexagon grid, resulting in a unique map of old forest proportion (OFP) for each dimension. Subsequently, we use spaceborne lidar data from NASA's Global Ecosystem Dynamics Investigation (GEDI) to reproduce each OFP map in a modeling framework designed to 1) assess the extent to which each dimension of forest oldness can be mapped at large spatial scales, and 2) identify biophysical GEDI variables related to each dimension of forest oldness. We estimate that only 2% of forest classified as old in any dimension satisfied the old criteria in all three dimensions. We found substantial spatial variation in the mapped OFP estimates across the three dimensions, highlighting how definition criteria impacts old-growth maps. We also found that physically old forests were more effectively mapped using GEDI data than functionally or temporally old forests, and that physically old forests were more structurally similar to one another than temporally or functionally old forests. Our modeling results indicate that while remote sensing may be best suited to mapping physical old-growth characteristics, definitions that rely solely on physical characteristics do not adequately represent old forests throughout the eastern US. We propose that future efforts to map old-growth with spaceborne remote sensing data may maximize utility through collaboration between western and indigenous old-growth experts to determine broad yet nuanced approaches that are appropriately tailored to the target variable of old forests. These efforts should balance explicit and ecologically relevant old-growth definitions specifically for mapping that can be linked to remotely sensed data, 2) appropriate spatial resolutions, and 3) flexible quantitative frameworks that encompass the complexities and heterogeneity of old forests.

1. Introduction

Considerable ecological research has focused on forests that are generally referred to as old-growth—forests with relatively old trees and characteristics that require a long time to develop (Frelich and Reich, 2003; Spies, 2004). Early old-growth studies by Western scientists were reliant on ground-based observations to analyze a single or small collection of sites within a localized region or specific forest type (Davis, 1996; Gaines et al., 1997; Tyrrell, 1998). Initial attempts to map old-growth conditions were also local, utilizing a combination of ground-based and remotely sensed data (e.g. Helmer et al., 2000; Falkowski et al., 2009; Hansen et al., 2014). As mapping efforts expand in

---

geographic extent, there is a growing need for data sources and methods that can identify old-growth across a variety of forest types and diverse environmental conditions at scale.

The use of spaceborne remote sensing in old-growth mapping is limited but evolving (e.g. Spracklen and Spracklen, 2019; Spracklen and Spracklen, 2021; Davis et al., 2022; DellaSala et al., 2022). High resolution optical time-series are not long enough to appropriately characterize stand level disturbances and forest longevity on the temporal scale of old-growth processes. Mapping efforts have instead used forest structure as a proxy for longevity and to identify biophysical conditions within known old forests. Presently, forest structure is most effectively measured by lidar systems such as airborne laser scanning (ALS) or spaceborne waveform lidars (ex. the Global Ecosystem Dynamics Investigation (GEDI)), or synthetic aperture radar (SAR) systems (ex. TanDEM-X or NISAR) (Krieger et al., 2007; Kellogg et al., 2020). The future of large scale old-growth mapping will likely involve multi-sensor fusion that merges different types of information related to forest structure and functioning derived from lidar, radar, or multispectral, hyperspectral, and stereo optical imagery at high spatial resolutions, and the integration of these data sets with forest inventory and dendroecology observations.

The evolution in old-growth mapping efforts has renewed debate over old-growth definitions. In this new context the question becomes: what exactly is being mapped? Old-growth cannot be detected directly via remote sensing, and instead must be inferred through modeled relationships between remotely sensed biophysical predictor variables and a response variable related to old-growth. This method requires the response variable to be defined precisely and consistently throughout the area being mapped. However, forests age in many different ways. Old forests are highly complex and dynamic, composed of gradients and interconnected processes with diverse manifestations based on forest type, natural disturbance regimes, human legacy on the landscape, site quality, topographic position, and climate (Pesklevits et al., 2011). The difficulty in appropriately representing old-growth diversity with a consistently defined response variable is perhaps the biggest challenge to old-growth mapping at large spatial scales (Hirschmugl et al., 2023).

The diversity of old forests has lead to agreement within the scientific community that a single unified old-growth definition is not possible nor preferable. There are many ideas regarding how old-growth could be defined based on both Western forest science and Traditional Ecological Knowledge from indigenous communities (Hilbert and Wiensczyk, 2007; Wirth et al., 2009). Recently, two different old-growth definitions were developed for the US Forest Inventory and Analysis (FIA) network that resulted in divergent estimates of how much old-growth exists throughout public lands in the US, despite using the same inventory data and estimation methods (Pelz et al., 2023; Barnett et al., 2023). These studies have advanced old-growth discourse in the US by developing standardized definitions that can be applied to FIA data at regional scales, and together the results suggest that old-growth amount estimates are highly sensitive to definition criteria. Neither Pelz et al. (2023) nor Barnett et al. (2023) released spatially explicit maps of old-growth, however one may assume that if produced, such maps would be substantially different based on the contrasting definition criteria.

In general, the inference that old-growth definitions have a large impact on old-growth maps is critical if spatially explicit old-growth information is used to inform forest management plans, resource extraction, or conservation efforts. Multiple old-growth definitions are useful to understand and contrast the spatial patterns of old forest characteristics as long as the definition differences are understood and recognized. Accordingly, a systematic comparison of the Pelz et al. (2023) and Barnett et al. (2023) definitions and resultant old-growth maps is necessary to contextualize the divergent estimates and to inform future old-growth investigations within the US. To do so, we propose the following conceptual framework to evaluate old forest definitions developed for the FIA network.

Forest attributes related to old-growth can be grouped into three categories, which we refer to as old-growth dimensions:

1. **Temporal**: tree ages and overall stand age structure, the number and age of cohorts (if applicable)
2. **Physical**: the size and shape of trees, stand stem density, basal area, biomass, canopy cover and vertical profile, structural complexity
3. **Functional**: biogeochemical processes such as net primary or ecosystem production (NPP, NEP) or nutrient cycling, etc.

These forest attributes change constantly over time, dependent on demographic processes (e.g. recruitment, growth, mortality) and disturbance regimes that shape these processes. Our framework simplifies changes in forest attributes by assuming development over time, such as from less to more biomass, or from a younger to an older maximum tree age. Forest oldness is then defined as the progression of a given attribute's value over time, and can be independently assessed with respect to each dimension (Fig. 1A). *In situ* forest stands within the FIA network can be classified as "old" or not along a given dimension by; 1) choosing a specific attribute representative of the dimension (ex. mean stand age), 2) setting a threshold value along its developmental gradient to designate the onset of oldness (ex. 120 years), and 3) comparing this value to those from inventoried forest stands (Fig. 1B). Importantly, classifications are neither mutually inclusive or exclusive across the dimensions. While this method conflicts with views of old-growth as a dynamic process instead of a developmental state that can be classified (e.g. Spies, 2004; Pesklevits et al., 2011; Barton and Keeton, 2018), it is useful in contrasting definition criteria, estimating the spatial patterns of old forests, and quantifying the extent to which various old-growth definitions can be mapped with remote sensing.

In this paper we contrast old-growth definition criteria from Pelz et al. (2023) and Barnett et al. (2023). We then evaluate the definitions with respect to old-growth mapping throughout the eastern US using data from the GEDI mission as a case study. Our goal is to systematically assess the impact of old-growth definition criteria on the amount of old forest estimated throughout the eastern US, and the ability to map old forests using GEDI data. In achieving this goal we seek to answer the following science questions:

1. What are the spatial patterns associated with eastern old forests and how do they vary by dimension?
2. To what extent can each dimension of old-growth be mapped within our framework using GEDI lidar data?
3. Are there specific structural characteristics associated to each dimension of old-growth?

We hypothesize that definition criteria impacts the extent to which an old-growth definition can be predicted and mapped using GEDI data, and will evaluate modeling success using normalized prediction error. We expect 1) the physical dimension of old-growth will be more effectively mapped with GEDI data than the temporal or function dimensions, and 2) that temporally and functionally old forests may also possess structural signatures that can be detected and leveraged for mapping. We intend the results of this study to inform the definition development and theoretical underpinnings of future old-growth mapping efforts.

2. Material and methods

We begin our analysis (Fig. 2) by integrating the old-growth definition criteria from Pelz et al. (2023) and Barnett et al. (2023) into the forest oldness conceptual framework (Fig. 1), and derived unique temporal, physical, and functional oldness definitions by forest type for the eastern US. We then classified every forest stand sampled by the FIA network as old or not according to each dimension's definition. From the classifications we produce areal estimates of old forest proportion (OFP) for each dimension, which represent the ratio of old forest area to total
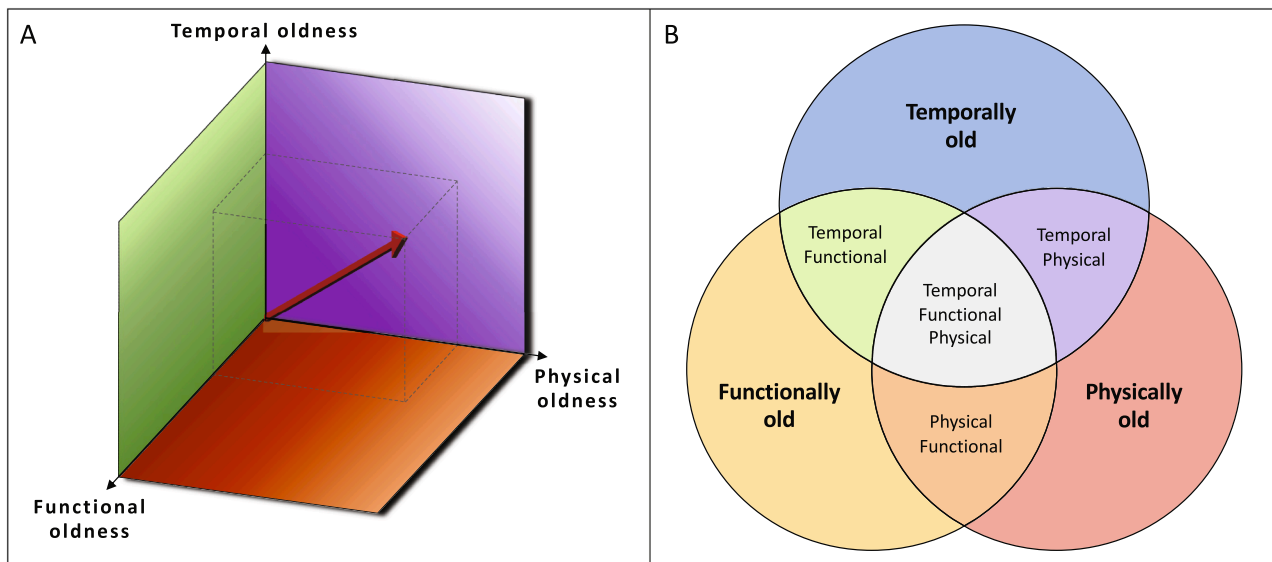
Fig. 1. (A) A theoretical framework for quantifying forest oldness along three dimensions: temporal, physical and functional. The red arrow represents how a forest stand's attributes could be mapped onto each dimension, and demonstrates that a stand's oldness in each dimension may not be equal. Threshold values can be set along each dimension (not shown here) to delineate the onset of old-growth characteristics for that dimension. Evaluating data from *in situ* stands against the threshold values results in a binary classification of forest oldness along each dimension, which are neither mutually inclusive nor exclusive. (B) Possible combinations of stand-level old-growth classifications when considering all three dimensions. A stand's classification in one dimension is independent from the other dimensions, in that physical characteristics are not be considered when classifying temporal oldness, and so on. There may or may not be multiple old-growth classifications across the dimensions for a given forest stand.
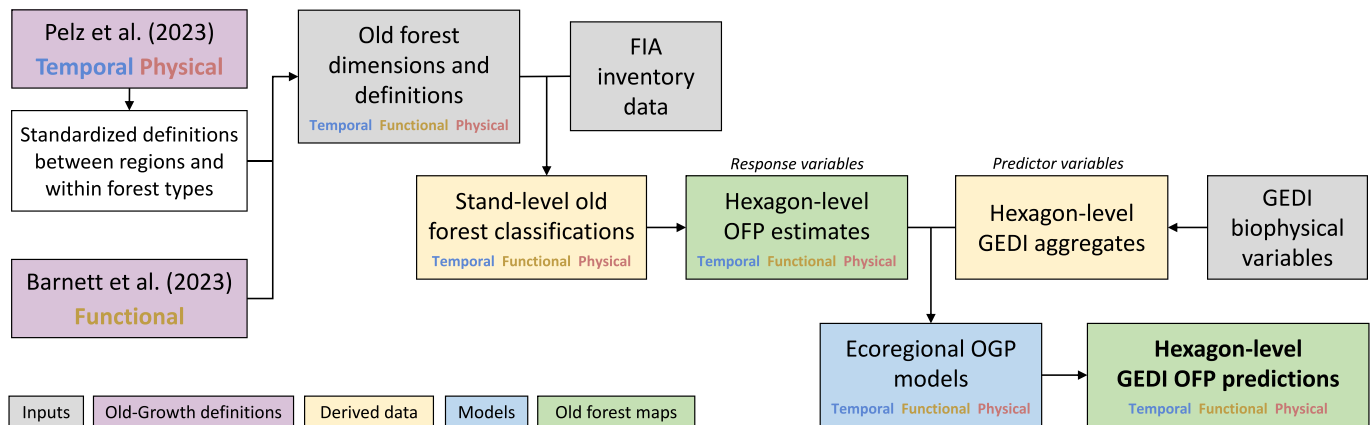
Fig. 2. Methodological overview: Old forest definitions from Pelz et al. (2023) from Barnett et al. (2023) were standardized within our conceptual oldness framework (Fig. 1) and applied to FIA inventory data resulting in binary old forest classifications at the stand-level across the temporal, functional, and physical old-growth dimensions. From these classifications, we estimated the old forest proportion as a ratio of old forest area to total forest area for each dimension, using ratio estimators adapted from Bechtold and Patterson (2005) applied within a hexagonal tessellation covering the eastern US. The result was three separate maps of OFP for eastern US forests. Footprint-level GEDI variables from forested land were then aggregated within the hexagonal grid and used as predictor variables in modeling the OFP estimates. Regression tree models were calibrated at the ecoregion level (Fig. 3) for each dimension's OFP estimates, resulting in GEDI-based prediction maps of OFP for each dimension. The variable importance from these models were compared to gain ecological inference about the structural characteristics of each old-g. rowth dimension.

forest area within an equal-area hexagonal tessellation of the land surface. We then assessed the extent to which each dimension's OFP estimates can be reproduced using biophysical forest attributes inferred from GEDI lidar forest structure measurements. We use regionally calibrated regression trees to model the OFP estimates for each old-growth dimension as a function of GEDI variables sampled from forested land and aggregated to the spatial resolution of the OFP estimates. Lastly, we determine which types of aggregated GEDI forest variables were most important in predicting each set of OFP estimates. The details of the analysis components are described in full in the following sections.

2.1. National forest inventory data

The FIA data used in this analysis were obtained from the plot and condition tables in the FIA database, for plots sampled between 2010 and 2022 (Gray et al., 2012). If an individual plot was sampled twice during this period, we used the most recent inventory information. Data were obtained and analyzed at the stand-level using the 'rFIA' package in 'R' (Stanke et al., 2020; R Core Team, 2022).

2.2. Old forest definitions

On April 20th 2023, the United States Forest Service (USFS) released

a national inventory of old-growth and mature forests within US federal lands (Barndt et al., 2023). Definitions were developed by USFS foresters and ecologists for predominant forest types within each of the nine Forest Health Protection regions within the US, and criteria identifying old-growth characteristics were set individually for different old-growth community types defined as a collection of FIA forest type groups. The definitions were designed specifically for FIA data, and an explanation of the definition development process is provided by Pelz et al. (2023). Here, we used the eastern and southern region definitions (respectively, Tables 15–17 in Barndt et al. (2023)) as the foundation for our temporal and physical old forest definitions. This required some standardization of old growth community types and definition criteria to ensure consistency in the application of old-growth definitions throughout our study region, as outlined below.

First, we standardized definition criteria for old growth community types that occurred in both regions (e.g. northern hardwoods). The standardization of definition criteria was done to ensure a single set of definition thresholds were used for community types that occurred in both regions. We also merged community types across the regions when the species compositions and definition thresholds were comparable based on our informed opinion of forest composition in eastern forests, and resulted in the merging of five community types.

Next, we harmonized the temporal and physical criteria for each community type across the regions. The southern and eastern regions used identical temporal criteria, in that stand age must exceed a threshold value, and we made no further modifications. The physical criteria however varied between regions. The eastern region used a minimum density of large trees, in which the density (ex. 10 trees per acre (0.405 ha)) and diameter of large trees (ex. 20 inches (0.508 m)) varied independently by community type. The southern region also required a minimum density of large trees, but the density was held constant at six trees per acre and while the size threshold for large trees was allowed to vary. There were also live basal area and standing dead

tree criteria included in the southern region definitions from Pelz et al. (2023). For simplicity, we opted to use the eastern region's definition criteria of physical forest oldness that only utilized a large tree density threshold, ignoring the basal area and standing dead requirements. We estimated the appropriate density and large tree threshold values for southern region forest types using data from Gaines et al. (1997). The result was a set of harmonized temporal (stand age) and physical (large tree density) oldness criteria for the old-growth community types set by Pelz et al. (2023) in the eastern US (Table 1).

Functional forest oldness criteria were taken directly from Table 2 in Barnett et al. (2023). In that work, the authors implemented a space-for-time substitution using FIA plot data to relate carbon accumulation to stand age for a combination of FIA forest type group and productivity classes, stating that functional old-growth characteristics are reached when stand-level aboveground carbon density reaches 95% of a theoretical maximum value derived from FIA stand data. The authors fit a Chapman-Richards growth model to characterize carbon accumulation over time as a function of stand age, and estimated parameters that minimized the models' normalized root mean square error. They then calculated the age at which functional old-growth characteristics were reached at the stand level for combinations of FIA forest type group and productivity class, substituting the estimated parameters into the growth equation and setting y equal to 95% of the asymptotic carbon density level. For a complete explanation of the functional old-growth definition, see Barnett et al. (2023). Here, we use the same exact forest types, productivity classes, and age thresholds calculated by Barnett et al. (2023) to classify functional oldness within our conceptual framework. We also performed a comparison of the mean temporal and functional age thresholds for eastern forests to aid in understanding estimate differences between the temporal and functional dimensions.

Table 1
Old-growth forest types and associated temporal and physical dimension thresholds, adapted from Pelz et al. (2023) and harmonized across the eastern and southern regions for consistency.

Short Name	Long Name	Region	FORTYPCD	STDAGE	TPA	DBH
Xeric Oak (N)	Dry oak	north	162, 163, 165, 167, 182, 184, 404, 405, 501, 502, 506, 507, 509, 510, 513, 515	100	20	16
Sub-boreal Spruce/Fir	Sub-boreal spruce/fir	north	122, 125	140	10	12
N. Pine	Northern pine	north	101, 102, 103	100	20	12
Beech/Maple/Basswood	Beech maple basswood	north	805	140	10	16
Wetland hardwood	Wetland hardwood	both	600, 608, 700, 701, 702, 703, 704, 705, 706, 707, 708, 709, 809, 962	120	10	18
Other	other	both		100	10	14
N. hardwood	Northern hardwood	both	517, 520, 800, 801, 802, 809	120	10	15
Montane Spruce/Fir	Montane spruce and spruce-fir	both	121, 123, 124, 128, 129, 902	120	10	15
Mesic Oak	Dry-mesic oak (S) + mesic northern oak (N)	both	500, 502, 503, 504, 505, 510, 511, 512, 515, 516, 519, 962	140	6	20
Conifer N. hardwood	Conifer northern hardwood	both	104, 105, 123, 124, 400, 401, 902	140	10	16
Xeric Pine, Pine/Oak	Xeric pine and pine-oak forest and woodland	south	162, 163, 165, 167, 171, 400, 402, 404, 405, 409, 500, 510, 514	100	10	10
Xeric Oak (S)	Dry and xeric oak forest, woodland, and savanna	south	500, 501, 502, 510, 514, 515, 519, 600, 962	90	10	8
S. wet Pine	Southern wet pine forest, woodland, and savanna	south	141, 142, 166, 400, 407	80	10	9
Coastal plain hardwood	Coastal plain upland mesic hardwood forest	south	600, 962	120	10	18
Seasonally wet hardwood	Seasonally wet oak-hardwood woodland	south	500, 504, 520, 600, 962	100	10	16
Dry-mesic Oak/Pine	Dry and dry-mesic oak-pine forest	south	161, 162, 163, 400, 404, 405, 406, 409	120	10	15
Mesophytic	Mixed mesophytic and western mesophytic forest	south	500, 506, 511, 516, 517, 800, 801, 805, 962	140	10	22
Longleaf/Slash Pine	Upland longleaf and south Florida slash pine forest, woodland, and savanna	south	141, 400, 403	80	10	13
Floodplain hardwood	River floodplain hardwood forest	south	500, 508, 600, 601, 602, 605, 705, 706, 708, 962	100	10	14
Eastern riverfront	Eastern riverfront forest	south	600, 700, 702, 703, 704, 705, 709, 962	100	10	20
Cypress/Tupelo swamp	Cypress-tupelo swamp forest	south	607, 609	120	10	8

Table 2

OFP estimates and 95% confidence intervals for each dimension of old-growth, and all possible dimensional combinations, for all eastern forests and by ecoregion.

Ecoregion	Temporal		Functional		Physical		T&F		T&P		F&P		All	
	OFP	CI	OFP	CI	OFP	CI	OFP	CI	OFP	CI	OFP	CI	OFP	CI
all	4.64	0.000733	6.51	0.00084	45.2	0.0017	1.07	0.000359	3.54	0.000648	5.13	0.000758	0.838	0.00032
Northern Forests (5.23)	5.81	0.00302	1.73	0.00169	37.5	0.00626	1.38	0.00152	3.27	0.00232	1.05	0.00133	0.803	0.00116
Central Mixedwood Plains (8.12)	3.37	0.00537	1.60	0.00376	40.2	0.0146	0.883	0.00285	2.10	0.00435	1.11	0.00318	0.632	0.00242
Southeastern Plains (8.3)	2.20	0.00135	10.1	0.00273	44.2	0.00449	0.788	0.000825	2.02	0.00131	8.27	0.00253	0.761	0.000816
Ozark-Ouachita-Appalachian (8.4)	8.71	0.00428	6.00	0.00344	56.9	0.00726	0.661	0.00122	7.59	0.00402	5.09	0.00322	0.587	0.00116
Atlantic and Coastal Plains (8.5)	4.13	0.00797	13.7	0.0136	50.1	0.0197	2.54	0.00632	3.39	0.00727	9.88	0.0119	2.090	0.00578
Temperate Prairies (9.2)	4.00	0.0604	1.69	0.0387	41.4	0.150	0.59	0.0249	2.85	0.0529	0.933	0.0297	0.407	0.0210

2.3. FIA stand classification

The temporal, physical and functional old forest definitions were applied to FIA inventory data at the stand level based on the FIA forest type associated with each stand. For the temporal and physical dimensions the forest type assignment is documented in Table 1, while for the functional dimension the forest type assignment was based on the combination of stand productivity class and FIA forest type group. An FIA stand is an identification of specific forest characteristics based on land use, reserve status, ownership, regeneration status, tree density, forest type and stand size within a plot, and there can be multiple stands located on a plot (Bechtold and Patterson, 2005). Each stand is assigned an age based on the average age (from tree cores) of two or three dominant canopy trees. It has been shown that stand age is not a reliable measure of the time since stand replacing disturbance, and should instead be interpreted as the mean age of the dominant diameter class within the stand (Stevens et al., 2016). In the case of multi-modal age distributions, the stand age variable may not appropriately reflect the overall stand age structure. This variable served as the basis for the temporal and functional old-growth dimensions. We calculated the physical old-growth dimension's large tree density for each stand using the tree-level inventory data and associated large tree size and density thresholds in Table 1. We then classified each FIA stand as old or not by comparing its values to the temporal, physical and functional thresholds. The result was a set of three old forest classifications for each stand.

2.4. Areal estimation of old forest proportion

From the binary stand-level old forest classifications, we estimated the proportion of old forest land relative to all forest land for each old-growth dimension, which we refer to as the old-forest proportion (OFP) estimates because values ranged between 0 and 1, inclusive. We adapted the ratio-of-means estimator from Section 4.3.4 of Bechtold and Patterson (2005), using the Horvitz-Thompson estimator to estimate both the numerator and denominator terms, as follows

$$\widehat{R}_j = \frac{\widehat{Y}_j}{\widehat{X}_j} = \frac{\frac{1}{n_j}\sum_{i=1}^{n} Y_{ij}}{\frac{1}{n_j}\sum_{i=1}^{n} X_{ij}}, \tag{1}$$

in which $\widehat{R}_j$ is the ratio estimate of old-growth forest area to total forest area for a given type, $\widehat{Y}$ and $\widehat{X}$ are the Horvitz-Thompson estimates of old-growth forest area and all forest area respectively, j is an index representing each spatial estimation unit, n_j represents the number of FIA plots within the spatial estimation unit, i is an index representing each individual FIA plot within spatial estimation unit j, Y_{ij} represents the proportion of each FIA plot that is classified as old-growth forest expressed as a unit interval [0,1], and X_{ij} represents the proportion of each FIA plot that is classified as forest expressed as a unit interval [0,1].

FIA plots frequently contain multiple condition classes, so to properly account for this possibility we calculated Y_{ij} by summing the plot-area proportions of all forested conditions classified as old-growth on each plot. Similarly, we calculated X_{ij} by summing the plot-area proportions of forested conditions on each plot.

To estimate the variance associated with $\widehat{R}_j$ we first calculated the variance associated with the Horvitz-Thompson estimates of $\widehat{Y}_j$ and $\widehat{X}_j$ as

$$\widehat{\sigma}_{Y_j}^2 = \widehat{Var}\left[Y_j\right] = \frac{1}{n_j(n_j-1)} \sum_{i=1}^{n_j} \left(y_{ij} - \widehat{Y}_j\right)^2 \tag{2}$$

$$\widehat{\sigma}_{X_j}^2 = \widehat{Var}\left[X_j\right] = \frac{1}{n_j(n_j-1)} \sum_{i=1}^{n_j} \left(x_{ij} - \widehat{X}_j\right)^2 \tag{3}$$

along with the covariance of $\widehat{Y}_j$ and $\widehat{X}_j$ in the form of

$$\widehat{\sigma}_{XY_j}^2 = \widehat{Cov}\left[XY_j\right] = \frac{1}{n_j(n_j-1)} \sum_{i=1}^{n_j} \left(x_{ij} - \widehat{X}_j\right)\left(y_{ij} - \widehat{Y}_j\right) \tag{4}$$

in which y_{ij} and x_{ij} are respective plot level values of proportion old-growth forest and total forest for plot i within spatial estimate unit j. We then used the variance and covariance to calculate the variance of $\widehat{R}_j$ as

$$\widehat{\sigma}_{Rj}^2 = \widehat{Var}\left[R_j\right] = \frac{1}{\widehat{X}_j^2}\left(\widehat{\sigma}_{Yj}^2 + \widehat{R}_j^2 \times \widehat{\sigma}_{Xj}^2 - 2 \times \widehat{R}_j \times \widehat{\sigma}_{XY_j}^2\right) \tag{5}$$

While slightly different from standard estimation procedures with FIA data that require post-stratification and strata weights (see Bechtold and Patterson (2005, 2018)), ratio estimation using a Horvitz-Thompson estimator has been shown to yield highly similar results to the post-stratified methods when estimating aboveground biomass density, and has the benefit of being easier to reproduce (May et al., 2023). The spatial estimation units were delineated by an equal-area hexagon tessellation grid covering the Eastern US (Fig. 3). This grid informs the FIA sampling design and is the highest spatial resolution for which estimates from FIA data should be made using the FIA's standard estimation methods (Menlove and Healey, 2020).

2.5. Old forest proportion modeling

There were two motivations for the second phase of our study involving OFP modeling using GEDI data, ordered here by importance; 1) to determine the extent to which the old forest definitions produced OFP estimates that could be modeled using GEDI data, and 2) to identify which GEDI variables were important in predicting each dimension's OFP estimates. Producing the most accurate predictions of OFP was not an objective, and as such we prioritized interpretability and ecological inference over maximizing map accuracy. We trained regression tree
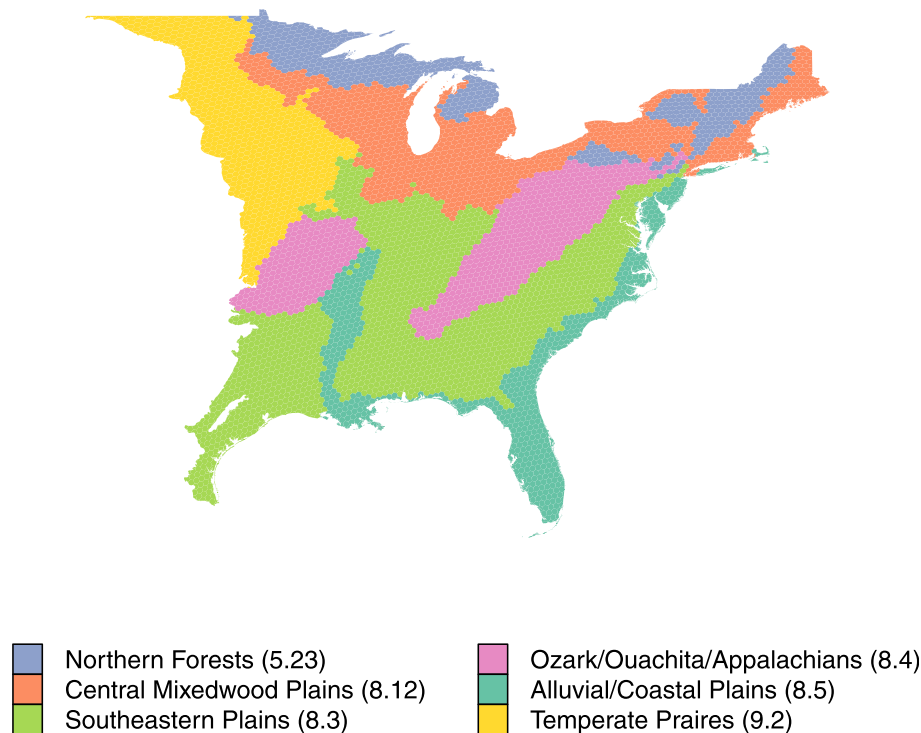
Fig. 3. The extent of eastern forests considered in this analysis, and the ecoregion delineations used in model calibration, which are based on the EPA level II ecoregions mapped onto the hexagon grid. EPA ecoregions 5.2 and 5.3, and 8.1 and 8.2 were combined based on size and similarity.

models using the 'R' package 'rpart', relating each old-growth dimension's OFP estimates to the aggregated GEDI variables (R Core Team, 2022; Therneau and Atkinson, 2022). Model fitting was performed individually within six different ecoregions, informed by the level II EPA ecoregion delineations within the Eastern US (Omernik and Griffith, 2014) mapped onto the hexagons (Fig. 3). The OFP estimates for each dimension of old-growth were the response variables, and the predictor variables were hexagon-scale biophysical forest attributes aggregated from the GEDI data within each hexagon. For each fitted model we summed the variable importance by variable type to determine an importance hierarchy that characterized which types of GEDI forest variables were most important in the models. The following subsections explain the steps of our OFP modeling exercise.

2.5.1. GEDI data

NASA's Global Ecosystem Dynamics Investigation is the first spaceborne mission designed to map forest structural attributes (Dubayah et al., 2020). GEDI is a multi-beam waveform lidar sensor that directly measured forest structure within footprints 25 meters wide, and was operational on the International Space Station from April 2019 - March 2023. GEDI's sole observable is a returned waveform, and throughout its first epoch GEDI is estimated to have collected 90 billion observations globally. From the waveform a suite of forest attributes are derived via signal processing and modeling, which are grouped into various data products. Here, we used GEDI footprint level 2A (L2A, canopy height) and 2B (L2B, canopy profile) data products collected between April 2019 and October 2022 (Dubayah et al., 2021a; Dubayah et al., 2021b). The GEDI mission produces a footprint level 4A (L4A, aboveground biomass) data product, however a recent analysis produced updated footprint level biomass models that produced predictions that were in better agreement with estimates from the FIA network, and these models were used in place of the official GEDI 4A data product (Bruening et al., 2023). We filtered the GEDI sample so that only observations over forest land were used, selecting only multi-modal waveforms (Hofton et al., 2019), and those that intersected a 30-meter resolution forest mask

(Wickham et al., 2021).

2.5.2. Predictor variables and dimensionality reduction

Hexagon-level aggregates of the GEDI metrics were used as the OFP model predictor variables. For each GEDI metric we calculated the mean, standard deviation, 50th, 75th, 95th and 99th percentiles at the hexagon level. We used L2A relative height metrics in 10 percentile increments from 10% to 90%, and 98%, which is a common proxy for maximum canopy height using GEDI data. The L2B canopy profile variables we used were percent canopy cover, plant area index (PAI), plant area volume density (PAVD), and foliage height diversity (FHD) (Hofton et al., 2019; Tang and Armston, 2019). We calculated partial PAI and plant area volume density (PAVD) variables specific to upper canopy foliage for each waveform. To calculate these upper-canopy metrics, we summed the PAI profiles and averaged the PAVD values for the upper half, third, quarter, fifth, and two-fifths of the canopy for each waveform, and then aggregated these values in the same manner as the other GEDI variables. Additionally, we used the number of modes in each waveform as a proxy for the number of canopy layers (Hofton et al., 2019). Lastly, we generated additional predictor variables for a select set of GEDI metrics by calculating the proportion of GEDI observations within each hexagon with values above specific threshold values (for example, the proportion of waveforms with a maximum canopy height above 35 meters). Combined, there were 205 candidate predictor variables used for model calibration. We organized the predictor variables by metric type into eight predictor variable groups for variable reduction prior to model fitting: biomass, percent canopy cover, FHD, canopy height, number of canopy layers, total canopy PAI, upper canopy PAI, and upper canopy PAVD.

GEDI metrics can be highly correlated with one another, and so we implemented a dimensionality reduction routine prior to fitting each OFP-ecoregion model. This routine minimized multicolinearity and decreased the overall number of predictor variables used to fit each model, and allowed us to assess which variable group was most important in predicting the OFP estimates (see Section 2.5.4). We applied the

following procedure to each of the eight variable groups separately. For each variable within a group we collected the within-group covariates with a correlation above 0.9, and selected the single predictor from that collection with the largest correlation to the OFP response variable. This process was repeated using the selected predictors within each group until all within-group correlations were below 0.9, resulting in a final set of variables for each group that minimized within-group correlations while maximizing correlations with the response variable. We then took the five variables with the strongest correlation to the response variable from each final set, to ensure each variable group had the same number of predictors allowed in model fitting. We allowed correlations above 0.9 between predictors in different groups as this information was valuable for ecological inference. Exactly 40 variables were used (five per group) in calibrating each model.

2.5.3. Model calibration

We calibrated 18 individual models based on the combination of old-growth dimension (three) and ecoregion (six). We used simple regression tree models as the outputs are interpretable and the variable importance scores are straightforward and comparable between models. We did not separate calibration data into testing and training sets, for several reasons. Excluding a subset of hexagons during calibration would preclude insight into which forest attributes were related to the OFP estimates in those hexagons, and generalizability was not a priority because the models were not applied to other hexagons not used in model training. We calibrated the models using hexagons with a forest proportion of at least 0.2 to reduce noise from those with little forest cover. Case weights were also assigned based on each hexagon's proportion forest, to ensure each hexagon's influence in the model was proportional to the amount of forest it contained. We used fivefold cross validation during calibration to determine a pruning length for each tree that minimized prediction error. We then allowed two additional splits in each model to improve the final predictions at the cost of some overfitting. Each calibrated model was then applied to the GEDI aggregates to predict OFP for that dimension within each ecoregion. Final predicted OFP maps for each old-growth dimension were produced by combining the predictions from all six ecoregions.

2.5.4. Model interpretation and inference

The 'rpart' model's variable importance measure reflects each predictor's ability to explain variation in the response variable (Therneau and Atkinson, 2022). We scaled the raw importance scores to assess each predictor variable's importance relative to all predictors in the model and summed the scaled scores for each predictor by variable group from Section 2.5.2. By limiting each variable group to only five predictors, we ensured a fair comparison of importance by group, otherwise groups with more than five predictors would have inflated importance measures relative to the other groups. This resulted in a measure that was comparable between old-growth dimensions for a given region, and between regions for a given oldness dimension, allowing inference into which variable groups were the best identifiers of each oldness dimension's OFP estimates. We also calculated a combined measure of variable importance for each old-growth dimension that represented all six regions by weighting each region's importance values by the amount of forested land, which allocated appropriate weight to regions with different amounts of forest and allowed inference for eastern forests as a whole.

3. Results

3.1. Old forest estimation and classification

Estimates of old forest proportion (OFP), derived exclusively from the FIA data, varied by dimension throughout eastern forests (Table 2). Physically old forests, those with a high density of large trees, were the most common at 45.2%. Functionally old forests, in which annual net

biomass change is presumed to be near zero, were less prevalent at 6.5%. Temporally old forests, with a relatively old mean stand age, were least common at 4.6%. Only 0.8% of eastern forests qualified as old in all three dimensions. The spatial patterns of OFP were mostly different between dimensions. The only areas with notable overlap in old forest hotspots between the temporal and physical dimensions occurred along the spine of the Appalachian Mountains and the Adirondack Mountains. Between the physical and functional dimensions, the only overlap occurred in the eastern Cross Timbers region(Fig. 4).

Regional trends in estimated OFP varied by dimension. Temporally old forests were most common in the Ozark-Ouachita-Appalachian region (8.7%) and the Northern Forests region (5.8%) and least common in the Southeastern Plains region (2.2%) and the Ozark-Ouachita-Appalachian region (3.4%). The southern regions (Southeastern Plains, Ozark-Ouachita-Appalachian Mountains, and Alluvial and Coastal Plains) combined for more than five times as much functionally old forest than the northern regions (Northern Forests, Central Mixedwood Plains, and Temperate Prairies), 9.4% compared to 1.7%, despite similar temporal (4.5% compared to 4.9%) estimates. A weaker latitudinal trend in physical estimates between the southern and northern regions was also present (49.0% compared to 38.7%).

Regarding old forest classifications, stands that were classified as physically old were unlikely to be classified as old in another dimension, whereas most stands that were classified as temporally or functionally old were likely to classified as old in at least one other dimension Fig. 5. When considering overlapping classifications, the likelihood of old forest classification increased if a stand was classified as old in another dimension, and further increased if that stand was classified as old in both other dimensions (Table 3). This effect was consistent across all dimensions, for eastern forests as a whole and when ecoregions were considered independently. Classification rates were highly variable across the old-growth dimensions within any given forest type, as well as across forest types within any given dimension (Table 4). Temporal and functional old forest rates by forest type were mostly below 10%, while physically old rates ranged from 14% to 91%.

The comparison of temporal and functional oldness age thresholds yielded similar mean values for eastern forests as a whole, however there were substantial differences by forest type (Table 5). The spatial pattern of mean age thresholds within the hexagon grid revealed a slight latitudinal trend in the temporal thresholds, and a much larger latitudinal trend in the functional thresholds (Fig. 6).

3.2. Old forest prediction

Physical OFP estimates were modeled with the most success (Fig. 7). When combining results from the regional models, the difference in physical old forest percent between the estimated and predicted values (RMSD) was 14.9 (using non-independent validation data), which relative to the mean estimate (nRMSE) was 32%, and the GEDI variables explained 43% of the variation in OFP estimates. The functional OFP models were relatively less successful, with respective RMSD and nRMSD values of 7.4 and 119%, and the GEDI variables explained 45% of the functional OFP estimate variation. The temporal models had respective RMSD and nRMSD values of 6.2 and 148%, and the GEDI variables only explained 29% of the variation in OFP estimates.

Model bias, defined as the mean difference between estimated and predicted OFP, for each dimension was near zero (top row in Table 6), and the OFP predictions represented large-scale spatial patterns of each type of old forests to varying degrees (Fig. 7). However, attenuation bias resulted in an inability to predict the magnitude of OFP hotspots, evidenced by obvious spatial patterns in the model residuals for each dimension. The temporal models exhibited negative bias for large estimates of OFP (Table 6) predominantly throughout the Appalachian and Adirondack Mountains and Mark Twain National Forest. In contrast, the functional OFP models were able to accurately identify some but not all hotspots of functionally old forests, most notably the New Jersey Pine
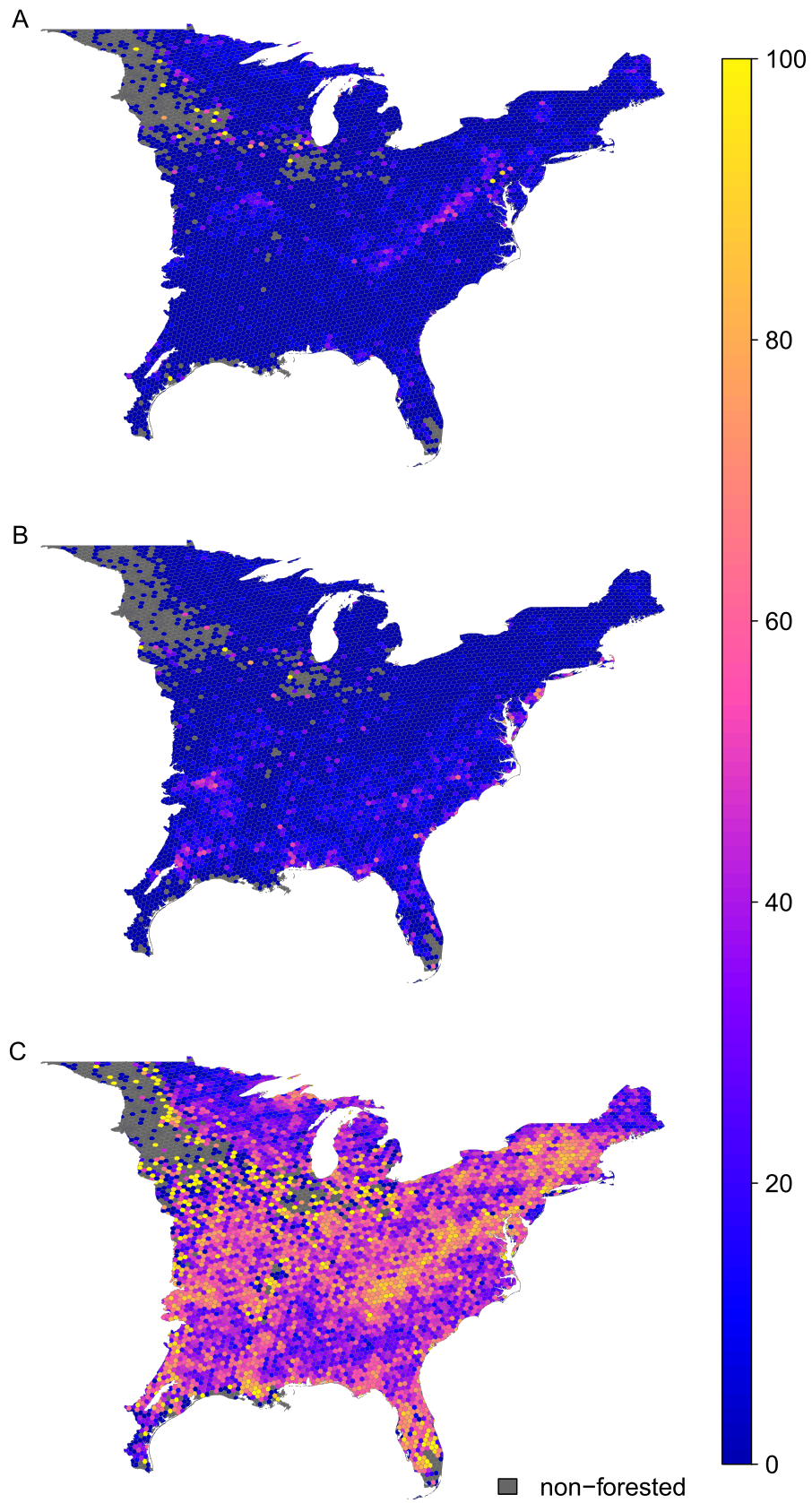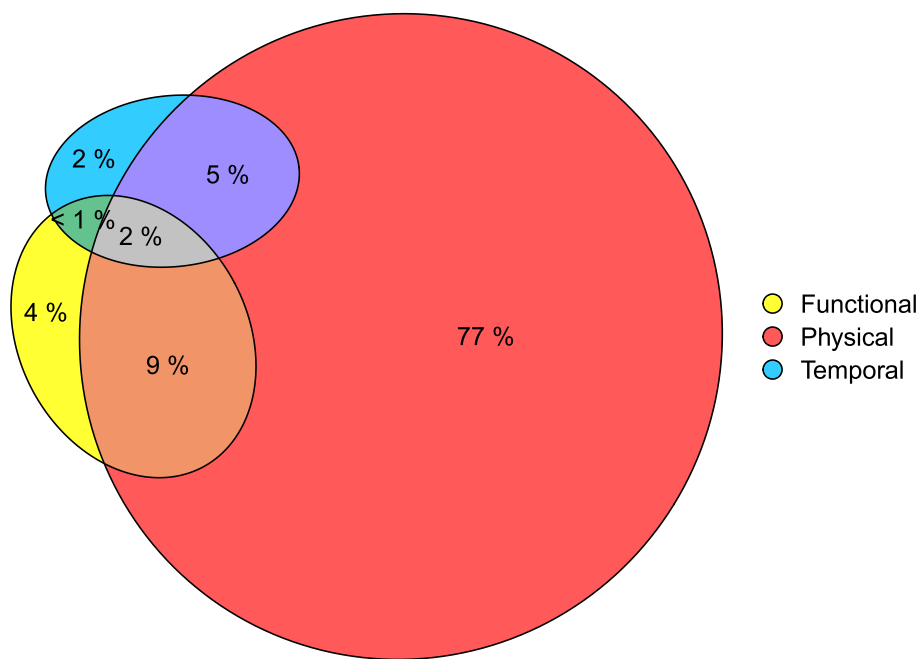
Fig. 4. Hexagon-level estimates of temporal (A), functional (B), and physical (C) old-growth proportion [0–1] mapped as a percentage [0–100] across the eastern US.

Fig. 5. Euler diagram of *in situ* old forest classifications at the stand level for all stands in the FIA network considered in this analysis; the empirical counterpart to the theoretical Fig. 1B. Percentages sum to 100, and thus represent the percent of stands classified relative to number of total stands with at least one old forest classification across the three dimensions.

Table 3
Stand-level rates of overlapping old-growth classifications (columns with '&'), along with baseline rates of classification for each dimension. For example, while 4.2% of all plots were classified as temporally old, 14.8% of functionally old plots were classified as temporally old, 7.6% of physically old plots were classified as temporally old, and 15.3% of functionally and physically old plots were classified at temporally old.

Region	Temporal	T&F	T&P	T&FP	Functional	F&T	F&P	F&TP	Physical	P&T	P&F	P&TF
All	4.20	14.8	7.56	15.3	6.44	22.6	11.8	23.8	40.0	72.0	73.1	75.7
Northern Forests (5.23)	5.43	79.6	8.89	76.3	1.55	22.7	24.7	31.9	52.3	59.1	56.7
Central Mixedwood Plains (8.12)	3.30	51.5	5.22	56.5	1.48	23.1	2.72	29.4	34.8	55.1	63.9	70.0
Southeastern Plains (8.3)	1.96	7.07	4.35	8.67	9.74	35.1	18.6	37.1	39.3	87.1	75.2	92.2
Ozark-Ouachita-Appalachian (8.4)	7.76	9.61	12.8	10.3	6.43	7.96	9.74	7.89	51.5	84.7	78.1	83.9
Atlantic and Coastal Plains (8.5)	3.89	17.7	6.56	20.3	13.5	61.1	20.1	62.1	46.1	77.8	68.8	79.1
Temperate Prairies (9.2)	3.84	27.3	6.38	33.3	1.76	12.5	2.35	12.3	35.8	59.4	47.7	58.3

Barrens, Ouachita National Forest, and Choctaw Nation. The physical OFP models were most successful in reproducing large-scale spatial patterns of physically old forests. These models tended to over-predict physical OFP on throughout the Allegheny plateau and western slopes of the Appalachian Mountains, the southeastern Peidmont region, and northwestern Great Lake states, while under-predicting throughout central New England, Adirondack Mountains, and eastern cross timbers region.

The GEDI variable types that best explained physically old forests were similar across ecoregions (Fig. 8); GEDI variables of foliage height diversity (FHD), a measure of canopy strata represented as a diversity index, aboveground biomass, and canopy height were consistently important predictors of physical OFP, while other variable types were comparatively unimportant. Functional OFP estimates were also best explained by variables related to canopy height and FHD, although there was not as much differentiation in importance across the variable groups as for the physical models. In contrast, temporal OFP model variable importance was the least differentiated by variable group for eastern forests as a whole, with substantial variation in importance across regions.

4. Discussion

Our analysis contrasts old forest dimensions and corresponding maps

of OFP. The OFP mapping results show that definition criteria has a strong and direct effect on the total estimates and spatial patterns of old forests. This finding helps reconcile estimate differences between Pelz et al. (2023) and Barnett et al. (2023). We infer that the spatial manifestation of old forest attributes is different for each dimension; in other words, large trees are not necessarily old, and old trees are not necessarily large. This inference is supported by relatively little overlap in OFP hotspots between the dimensions (Fig. 4) and the result that, as defined in this study, most physically old stands were not classified as functionally or temporally old (Fig. 5). This is not a new discovery, but adds further support to the idea that tree longevity and size are not directly related (Piovesan and Biondi, 2021). These results demonstrate how multiple definitions are useful in characterizing multifaceted old-growth conditions by mapping and contrasting the spatial patterns of old forests.

4.1. Old-growth definitions and mapping

The OFP modeling exercise revealed a hierarchy with respect to old forest mapping using structure derived from remote sensing (GEDI); physical OFP maps were modeled with the most success, functional OFP maps were modeled with relatively less success, and temporal OFP maps were not modeled effectively (Fig. 7). The mapping hierarchy supports our hypothesis that definition criteria impacts the extent to which an

Table 4

Stand-level old-growth classification rates for each dimension of old-growth and all possible combinations, grouped by all eastern forests, ecoregion, USFS old-growth community type from Pelz et al. (2023), and FIA forest type group from Barnett et al. (2023).

	Group	Source	Temporal	Functional	Physical	T&P	T&F	F&P	All
1	all	NA	4.2	6.44	40.02	3.02	0.95	4.71	0.72
2	Northern Forests (5.23)	ecoregion	5.43	1.55	31.92	2.84	1.23	0.92	0.7
3	Central Mixedwood Plains (8.12)	ecoregion	3.3	1.48	34.81	1.82	0.76	0.95	0.53
4	Southeastern Plains (8.3)	ecoregion	1.96	9.74	39.29	1.71	0.69	7.32	0.63
5	Ozark-Ouachita-Appalachian (8.4)	ecoregion	7.76	6.43	51.52	6.57	0.62	5.02	0.52
6	Atlantic and Coastal Plains (8.5)	ecoregion	3.89	13.46	46.13	3.03	2.38	9.25	1.88
7	Temperate Prairies (9.2)	ecoregion	3.84	1.76	35.75	2.28	0.48	0.84	0.28
8	Beech/Maple/Basswood	Pelz 2023	0.18	0.09	42.98	0.14	0.05	0.05	0.05
9	Conifer N. hardwood	Pelz 2023	3.97	11.17	63.26	3.67	3.16	10.21	3.01
10	Cypress/Tupelo swamp	Pelz 2023	4.41	4.53	87.34	4.3	1.39	4.41	1.28
11	Eastern riverfront	Pelz 2023	6.52	0	41.3	6.52	0	0	0
12	Floodplain hardwood	Pelz 2023	2.07	0.97	51.57	1.78	0.6	0.89	0.55
13	Longleaf/Slash Pine	Pelz 2023	11.28	1.03	40.51	9.74	1.03	1.03	1.03
14	Mesophytic	Pelz 2023	0.22	0.51	14.16	0.15	0.07	0.22	0
15	Mesic Oak	Pelz 2023	0.7	0.85	39.95	0.6	0.38	0.74	0.33
16	Dry-mesic Oak/Pine	Pelz 2023	0.06	15.53	27.77	0.03	0.05	10.41	0.02
17	Montane Spruce/Fir	Pelz 2023	2.39	1.63	16.74	1.1	1.63	0.91	0.91
18	N. hardwood	Pelz 2023	2.14	0.36	43.88	1.84	0.34	0.31	0.29
19	N. Pine	Pelz 2023	7.43	0.64	42.59	5.29	0.64	0.49	0.49
20	Other	Pelz 2023	7.69	3.7	22.93	3.56	1.78	1.82	1.01
21	Sub-boreal Spruce/Fir	Pelz 2023	1.54	1.98	14.36	0	1.54	0	0
22	Seasonally wet hardwood	Pelz 2023	20.27	0.74	62.43	14.28	0.74	0.59	0.59
23	Wetland hardwood	Pelz 2023	1.65	0.51	20.31	0.55	0.29	0.2	0.07
24	S. wet Pine	Pelz 2023	8.75	33.4	68.79	8.13	8.19	30.6	7.62
25	Xeric Oak (N)	Pelz 2023	23.55	12.7	22.91	9.73	2.37	1.13	0.76
26	Xeric Oak (S)	Pelz 2023	24.29	0.29	91.78	23.87	0.29	0.29	0.29
27	Xeric Pine, Pine/Oak	Pelz 2023	3.81	35.74	75.13	3.56	1.77	30.59	1.67
28	Aspen/Birch	Barnett 2023	0.99	0	17.88	0.74	0	0	0
29	Elm/Ash/Cottonwood	Barnett 2023	2.03	0.36	27.21	0.78	0.3	0.11	0.08
30	Fir/Spruce/Mountain Hemlock	Barnett 2023	0	0	0	0	0	0	0
31	Loblolly/Shortleaf Pine	Barnett 2023	0.65	26.93	31.32	0.43	0.65	18.1	0.43
32	Longleaf/Slash Pine	Barnett 2023	8.29	34.78	67.64	7.67	8.29	31.89	7.67
33	Maple/Beech/Birch	Barnett 2023	2.49	0.31	50.43	2.22	0.3	0.28	0.28
34	Oak/Gum/Cypress	Barnett 2023	2.45	2.08	49.35	2.2	0.99	1.85	0.89
35	Oak/Hickory	Barnett 2023	5.94	0.66	43.37	4.62	0.4	0.52	0.3
36	Oak/Pine	Barnett 2023	2.67	5.6	52.86	2.29	0.97	5.03	0.9
37	Spruce/Fir	Barnett 2023	13.45	4.25	19.18	5.16	4.13	1.96	1.96
38	Tropical Hardwoods	Barnett 2023	2.56	0	38.46	1.28	0	0	0
39	White/Red/Jack Pine	Barnett 2023	7.93	1.97	48.41	6.05	1.73	1.79	1.55

old-growth definition can be mapped using GEDI data within our modeling framework. We expect GEDI's height, biomass, and foliage height diversity (FHD) to be directly related to the density of large trees within a stand, so it is not surprising that the physical dimension is mapped most effectively and consistently. Relative consistency in variable importance across the regions (Fig. 8) suggests a higher degree of structural similarity in physically old forests throughout the eastern US than for temporally or functionally old forests.

In contrast, the temporal OFP models had relatively weak predictive power and a large combined nRMSD (Fig. 7), with considerable inter-regional differences in variable importance (Fig. 8). From these results we infer that temporally old forests do not have a strong and consistent structural signature that is different from temporally young forests when aggregated across space and forest types, which is contrary to our expectation. We propose three related explanations for this finding. First, old trees in the eastern US come in many different shapes and sizes (Pederson, 2010). The structure of temporally old forest stands likely varies spatially within and between these ecoregions, may be specific to individual forest types, and could also be dependent on a suite of environmental covariates not considered in our analysis. Thus mixing old forest classifications across forest types within a hexagon during our estimation process may weaken the overall signal between GEDI structural attributes and old forest prevalence if the structural signatures of old forests are different across forest types. Second, the FIA's stand age variable does not reflect the entire age structure of a stand, nor is it guaranteed to indicate the time since stand replacing disturbance, which may add uncertainty or noise to existing structure-age relationships.

Third, we speculate that sensitivity to structural attributes of temporally old forests is diminished by the spatial scale of our prediction framework, as localized high resolution analyses of old-growth forests have identified numerous age-dependent relationships to remote sensing data (Falkowski et al., 2009; Kane et al., 2010; Pinto et al., 2012; Martin et al., 2021). Our estimation process produces ratio estimates of old forests that represent an expanse of forested land that is very large, and most hexagons contain very low, if any, ratios of old forest. A smaller hexagon grid would result in more variation in the OFP estimate and may help to amplify a common structural signal within temporally old forests that may by currently overwhelmed within our current framework, however this hexagon grid is finest resolution recommended for areal estimation with FIA plot data (Menlove and Healey, 2020).

The modeling results for functionally old forests were mixed in that predictive power was in between that of the physical and temporal models, but there was not consistency across ecoregions in the GEDI attributes related to functionally old forests. Despite the temporal and functional dimensions' shared usage of stand age as a definition criterion (albeit with different thresholds), GEDI variables were able to explain variations in functional OFP more than variations in temporal OFP. This suggests a structural signal is at least somewhat present within functionally old forests. An explanation for this could be that functional oldness—the age at which stand biomass accumulation is presumed to be near zero—represents the onset of a forest condition with more structural consistency than temporal oldness. A recent analysis of GEDI data colocated with FIA plot data indicated both FHD and maximum canopy height as strong indicators of carbon storage capacity on FIA

Table 5
Mean temporal and functional old-growth age thresholds and the mean and median difference defined as the temporal threshold minus the functional threshold, by ecoregion, and both Pelz et al. 2023 and Barnett et al. 2023 groupings. Values were rounded to the nearest year, resulting in occasional discrepancies in the mean difference by one year.

Group	Source	Temporal	Functional	mean difference	median difference
all	NA	117	115	1	−10
Northern Forests (5.23)	ecoregion	117	147	−30	−24
Central Mixedwood Plains (8.12)	ecoregion	123	138	−15	−15
Southeastern Plains (8.3)	ecoregion	115	89	26	26
Ozark-Ouachita-Appalachian (8.4)	ecoregion	119	124	−5	−13
Atlantic and Coastal Plains (8.5)	ecoregion	106	89	17	19
Temperate Prairies (9.2)	ecoregion	117	138	−21	−19
Beech/Maple/Basswood	Pelz 2023	140	146	−6	−4
Conifer N. hardwood	Pelz 2023	140	114	26	22
Cypress/Tupelo swamp	Pelz 2023	120	121	−1	−15
Eastern riverfront	Pelz 2023	100	128	−28	−39
Floodplain hardwood	Pelz 2023	100	118	−18	−17
Longleaf/Slash Pine	Pelz 2023	80	111	−31	−21
Mesophytic	Pelz 2023	140	126	14	8
Mesic Oak	Pelz 2023	140	133	7	8
Dry-mesic Oak/Pine	Pelz 2023	120	50	70	76
Montane Spruce/Fir	Pelz 2023	120	140	−20	−14
N. hardwood	Pelz 2023	120	140	−20	−24
N. Pine	Pelz 2023	100	129	−29	−38
Other	Pelz 2023	100	149	−49	−78
Sub-boreal Spruce/Fir	Pelz 2023	140	130	10	6
Seasonally wet hardwood	Pelz 2023	100	133	−33	−32
Wetland hardwood	Pelz 2023	120	132	−12	−19
S. wet Pine	Pelz 2023	80	47	33	38
Xeric Oak (N)	Pelz 2023	100	125	−25	−32
Xeric Oak (S)	Pelz 2023	90	140	−50	−42
Xeric Pine, Pine/Oak	Pelz 2023	100	78	22	26
Aspen/Birch	Barnett 2023	103	178	−75	−78
Elm/Ash/Cottonwood	Barnett 2023	116	133	−17	−19
Fir/Spruce/Mountain Hemlock	Barnett 2023	100	428	−328	−326
Loblolly/Shortleaf Pine	Barnett 2023	116	41	76	76
Longleaf/Slash Pine	Barnett 2023	80	42	38	38
Maple/Beech/Birch	Barnett 2023	124	147	−23	−24
Oak/Gum/Cypress	Barnett 2023	109	116	−6	−15
Oak/Hickory	Barnett 2023	123	133	−9	−12
Oak/Pine	Barnett 2023	112	99	13	19
Spruce/Fir	Barnett 2023	118	127	−9	3
Tropical Hardwoods	Barnett 2023	100	146	−46	−46
White/Red/Jack Pine	Barnett 2023	106	130	−23	−18
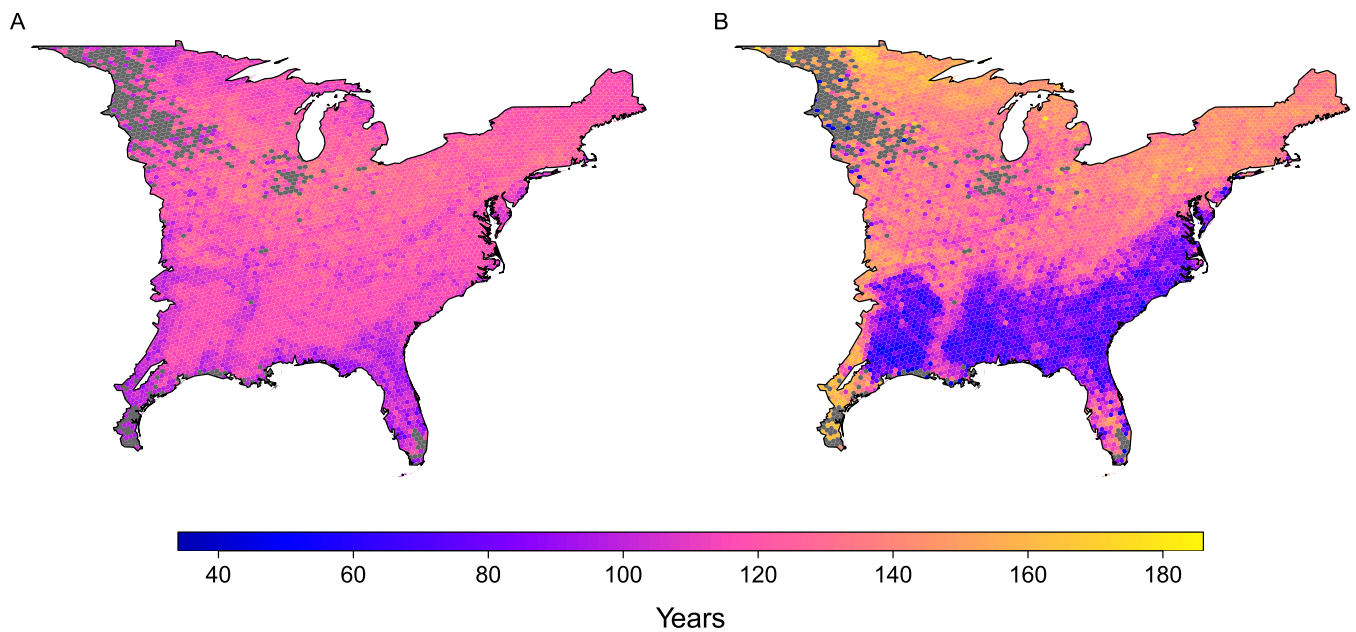
Fig. 6. Mean stand age threshold values by hexagon for the temporal (A) and functional (B) old-growth definitions.
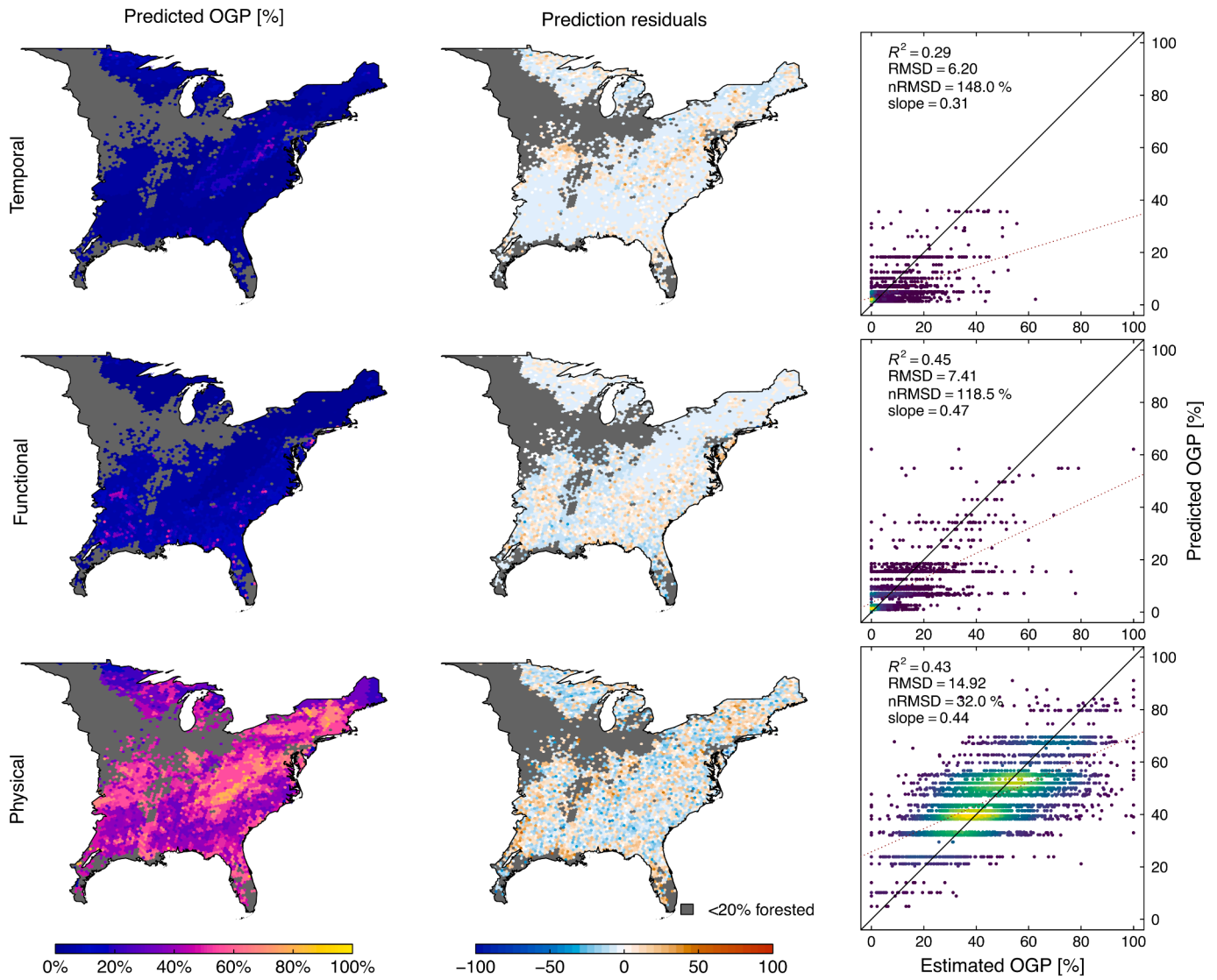
Fig. 7. OFP model prediction and residual maps and scatter plots of predicted (from GEDI) vs. estimated (from FIA) OFP values, combined across all ecoregions for each dimension of old-growth. The OFP prediction map units are percentages, and the residual maps units are the difference in percentage points (not a percent difference) between the estimated and predicted value. The solid dashed in the scatter plots is the 1:1 line, and the dark red dotted line is the trend line between the estimated and predicted values, the slope of which is reported along with the R^2, RMSD and normalized RMSD as a percent of the mean OFP estimate.

Table 6

OFP model bias, defined as the mean difference between estimated and predicted OFP, combined across ecoregions for each dimension. The values are in percentage points, so a value of 14.2 means the models under-predicted OFP relative to the estimated value by 14.2 points. Bias is reported for all predictions in each dimension (top row), as well as segmented by ranges of estimated OFP to assess model bias as a function of estimated OFP. The number of model data points (hexagons) within each range is represented by N for each dimension.

OFP range	Temporal		Functional		Physical	
	Bias	N	Bias	N	Bias	N
0–100%	0.0167	3941	−0.257	3941	0.313	3941
0–10%	−1.8	3347	−2.59	3059	−21	107
10–20%	7.76	427	4.48	556	−16	224
20–30%	14.2	107	11	176	−12.3	485
30–40%	18	36	12.4	86	−6.19	738
40–50%	22.3	19	18.3	36	−0.76	738
50–60%	28.2	4	20.2	16	4.92	636
60–70%	60.5	1	36.7	5	10	492
70–80%	-	-	35	6	16.5	323
80–90%	-	-	37.9	1	30.7	52
90–100%	-	-	-	-	21.5	146

plots (Crockett et al., 2023). These findings corroborate the result that FHD and canopy height were somewhat effective predictors of functional oldness (Fig. 8), given that functionally old forests should be near the maximum carbon storage capacity (Barnett et al., 2023). However, we did not find consistency in variable importance across ecoregions for functional OFP prediction, suggesting that while functional old-growth characteristics may be detectable via remote sensing, there is not same degree of structural consistency throughout functionally old forests as there is for physically old forests.

4.2. Age-based old-growth definitions

An old-growth definition characterized by near-equilibrium conditions with respect to biomass development is antithetical to views of old-growth as a dynamic and cyclical forest process that is "heterogeneously heterogeneous", rather than an end-state (Pesklevits et al., 2011). Nonetheless, the functional definition's age thresholds are valuable for identifying forests that are approaching maximum carbon storage capacity, and we argue a diversity of viewpoints as to what constitutes old-growth is beneficial for scientists or land managers defining old-growth
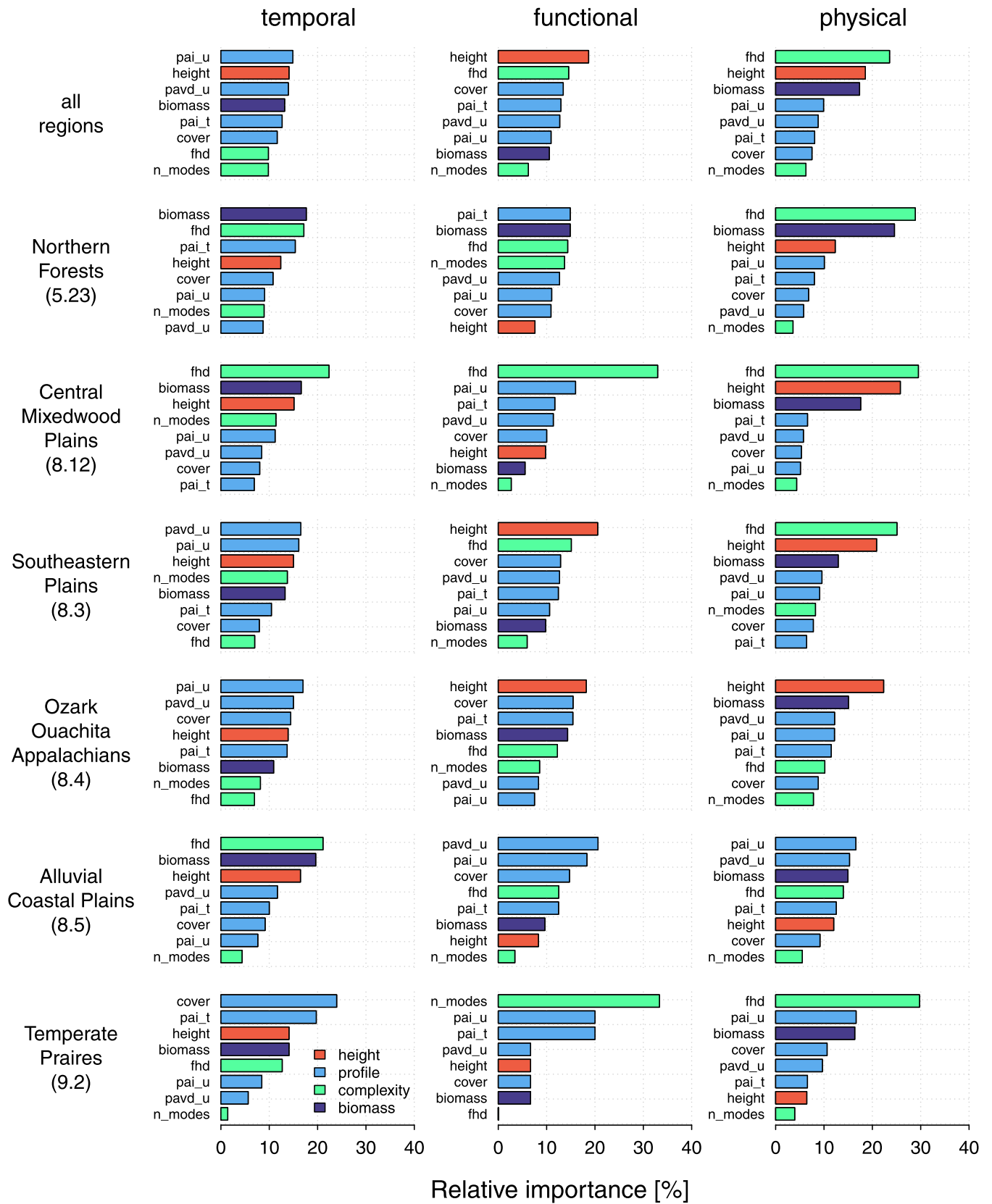
Fig. 8. OFP model variable importance scores aggregated by variable type and colored by biophysical attribute category, by ecoregion. The top row is a weighted measure of variable importance across all regions based on the ecoregions' relative proportions of forest.

for a specific use case or region, and is especially relevant when assessing old-growth dimensions for specific forest types. For example, observations of late successional biomass development within temporally old northern hardwood stands show that functional oldness may not be realized until long after temporal and physical oldness (Keeton et al., 2011), while surprisingly young ages of functional old growth reported by Barnett et al. (2023) demonstrate the opposite may be true for longleaf and shortleaf pines and other predominately southern forest types (Table 5). The spatial pattern of differences between the temporal and functional age thresholds (Fig. 6) explains latitudinal differences between the temporal and functional OFP estimates (Fig. 4). However, we did not directly investigate reasons for the latitudinal gradient in mean onset age of functional oldness. Yet, tree longevity and growth rates are known to be inversely related (Körner, 2017), and growth rates in lower latitude forests tend to be larger than those in northern latitude forests (Gillman et al., 2015). Together, these phenomena could explain the latitudinal gradient in mean onset of functional old-growth characteristics and differences relative to the mean temporal age thresholds (Fig. 6).

The temporal and functional age thresholds represent fundamentally different forested conditions; the functional thresholds estimate the age at which net carbon accumulation is near zero, while the temporal thresholds seem to identify a stand age old enough to suggest the absence of recent and widespread human activity within the stand. However, the FIA's stand age variable is an imperfect measure of age structure, and stands that originated from land use transitions in the early 19th century could have a mean stand age value above the temporal oldness thresholds. The nature of the FIA stand age variable precludes a direct mapping to the age ranges from Gaines et al. (1997) and Tyrrell (1998) which underpin the temporal thresholds, and helps explain the possibility that temporally old stands could have originated from land-use transitions. Furthermore, both the temporal and functional age thresholds appear relatively permissive when compared to other age-based definitions; Mosseler et al. (2003) suggest old-growth is achieved when the average age of dominant species equals about half its maximum longevity, as well as the presence of old trees approaching their species' maximum longevity. Nonetheless, the comparison of temporal and functional age thresholds raises an interesting and important question; at what point should forests that long ago regenerated after human-induced land use transitions be considered within old-growth discussions? Such forests are commonly referred to as mature, but at what point does a mature stand become eligible for old-growth status? According to definitions in which widespread human activity precludes old-growth status forever, most of today's forests can never become old-growth. Conversely, Pesklevits et al. (2011) suggest that time since disturbance should matter more than the type of disturbance, as long as enough time has passed and forest complexity and heterogeneity is allowed to develop. In this context, the marriage of remote sensing data and forest simulation models that track land use transitions and forest regrowth could help identify data driven answers to this question and assist in mapping of old forest attributes (Caspersen et al., 2000; Hurtt et al., 2011; Ma, 2021).

4.3. Conclusions and recommendations

Each dimension of forest oldness attempts to identify a forested condition that takes a long time to develop. However, physically old stands were far more common than temporally or functionally old stands, which suggests that physically old characteristics are achieved sooner in stand development than temporally or functionally old characteristics. From this we infer that physical thresholds alone are ineffective as an old-growth definition. This inference is in agreement with the approach of Pelz et al. (2023), in that both physical and temporal criteria were used to define old-growth. An argument could also be made that physically-based definition criteria limit the effectiveness of old-growth definitions. Old trees are not necessarily large, and definitions

that reflect a Euro-American colonialist perspective of towering "cathedral" forests more than likely ignore other manifestations of old forests appreciated by other worldviews (Moore and Nelson, 2023). Indeed, many of today's oldest eastern forests contain trees that are relatively short and gnarled in stature, passed over for logging or clearing for agricultural due poor site quality and accessibility issues (Davis, 1996). Therrell and Stahle (1998) even developed a spatially explicit predictive model to map old-growth based on steep and infertile soils that was 74% accurate in identifying old-growth stands in the Cross Timbers ecosystem in northern Oklahoma.

In contrast, the physical dimension of oldness as defined may provide more utility than the functional or temporal dimension from a strictly-mapping perspective. Our modeling results suggest that old-growth definitions related to physical oldness may be more effectively mapped than definitions that do not incorporate a physically-based component. However, in the view that old-growth forests must contain very old trees, the temporal dimension alone is the most meaningful. In this interpretation, our results suggest a potential trade-off with respect to ecological relevance and mapability of old-growth definitions: arguably the most important part of any old-growth definition—the presence of very old trees—is also the most difficult to precisely identify across large geographic extents within our prediction framework.

While this trade-off presents a challenge to old-growth mapping, it also provides exciting opportunities for discovery and collaboration between ground-based forest ecologists, Traditional Ecological Knowledge experts, and remote sensing scientists. Collaborations may be particularly helpful in balancing the interactions between components of a mapping analysis. It is our view that the challenge of appropriately mapping old-growth requires the consideration of at least four interrelated factors: 1) clearly stated definitions, 2) remote sensing and other
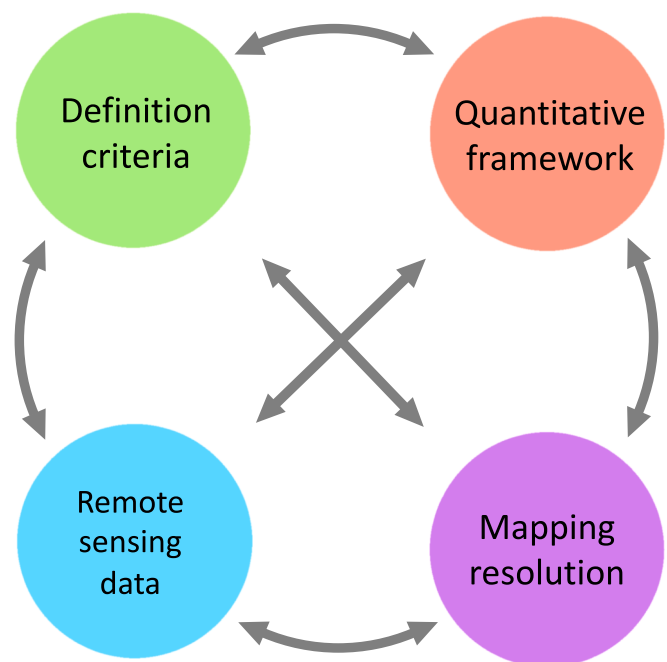
Fig. 9. Considerations that must be balanced within old-growth mapping analyses, as each factor necessarily impacts the others. For example, old-growth definitions may be developed by blending knowledge from western forest ecologists and traditional ecological knowledge from indigenous communities, and these definitions may necessitate a specific modeling approach or spatial resolution. Alternatively, the spatial resolution of a specific old-growth definition might impact the quantitative framework used to make predictions or identify old-growth conditions, and could impact which remote sensing data types were used as predictors. These examples are not exhaustive, and are provided to demonstrate the holistic nature of old-growth mapping.

spatial predictor data, 3) the spatial resolution at which old-growth conditions are mapped, and 4) the inferential framework and quantitative methods used to generate the map. In this conceptual model (Fig. 9) each component impacts and depends on the others, necessitating a holistic approach. We recommend that mapping efforts should resist the temptation to classify old forests, as this approach reduces complexity and introduces arbitrariness (Gray et al., 2023). Instead, analytic frameworks should recognize the heterogeneity inherent to old-growth structure, function, and composition. Emphasis be placed on generating a diverse stack of remotely sensed predictors that incorporate other forest attributes in addition to vertical structure. Furthermore, the native resolution of many remote sensing instruments is likely too fine to adequately characterize old-growth processes that operate at the community level within forests, as a single individual tree crown could feasibly cover the entire area of a Landsat or Sentinel pixel or GEDI observations. Instead mapping analyses may consider distributions of high-resolution spatial data (meters) within larger areas (hectares to square kilometers) that are more relevant to old-growth processes at the landscape scale. Such efforts may retain more information about the complexity and heterogeneity of forest attributes necessary for inference into old forest conditions and processes, compared with high-resolution pixel-level classification. Lastly, spatially explicit forest gap models that simulate demography and succession constrained by climatic, edaphic, topographic, and remotely sensed forest structure data hold great promise, as a calibrated simulation environment is well suited for investigating the many and diverse manifestations of forest change over very long time periods.

Author contributions

JB led the conceptualization and design of the study, with supervision from RD and input from NP, BP and LC. JB led the methodology and software development, data curation and formal analysis, and wrote the original draft of the manuscript with input from RD and NP. RD and BP acquired funding support. All authors contributed to the review and editing of the submitted manuscript.

Data statement

All FIA and GEDI data used in this manuscript are freely and publicly available. Products (maps, models, code) produced in the analysis are available upon request from Ralph Dubayah.

Declaration of Competing Interest

The authors declare that they have no known competing financial interests or personal relationships that could have appeared to influence the work reported in this paper.

Data availability

All input data are publicly available and the analysis outputs will available upon request from Ralph Dubayah

Acknowledgements

References

Barndt, S., Gray, A., Hayward, G., Hiemstra, C., Kamoske, A., Kleinsmith, S., Krueger, J., Palmer, M., Pelz, K., Salverson, W., Schuler, T., Schumacher, C., Tilton, K., Woodall, C., 2023. Mature and old-growth forests: definition, identification, and initial inventory on lands managed by the forest service and bureau of land management.

Barnett, K., Aplet, G.H., Belote, R.T., 2023. Classifying, inventorying, and mapping mature and old-growth forests in the united states. Front. For. Global Change 5, 1070372.

Barton, A.M., Keeton, W.S., 2018. Ecology and Recovery of Eastern Old-Growth Forests. Island Press.

Bechtold, W.A., Patterson, P.L., 2005. The enhanced forest inventory and analysis program–national sampling design and estimation procedures. Number 80. USDA Forest Service, Southern Research Station.

Bruening, J.M., May, P.B., Armston, J.D., Dubayah, R.O., 2023. Precise and unbiased biomass estimation from gedi data and the us forest inventory. Front. For. Global Change 6, 1149153.

Caspersen, J.P., Pacala, S.W., Jenkins, J.C., Hurtt, G.C., Moorcroft, P.R., Birdsey, R.A., 2000. Contributions of land-use history to carbon accumulation in us forests. Science 290 (5494), 1148–1151.

Crockett, E.T., Atkins, J.W., Guo, Q., Sun, G., Potter, K.M., Ollinger, S., Silva, C.A., Tang, H., Woodall, C.W., Holgerson, J., et al., 2023. Structural and species diversity explain aboveground carbon storage in forests across the united states: evidence from gedi and forest inventory data. Remote Sens. Environ. 295, 113703.

Davis, M.D., 1996. Eastern Old-Growth Forests: Prospects for Rediscovery and Recovery. Island Press.

Davis, R.J., Bell, D.M., Gregory, M.J., Yang, Z., Gray, A.N., Healey, S.P., Stratton, A.E., 2022. Northwest forest plan—the first 25 years (1994–2018): status and trends of late-successional and old-growth forests. Technical report.

DellaSala, D.A., Mackey, B., Norman, P., Campbell, C., Comer, P.J., Kormos, C.F., Keith, H., Rogers, B., 2022. Mature and old-growth forests contribute to large-scale conservation targets in the conterminous united states. Front. For. Global Change 5, 979528.

Dubayah, R., Blair, J.B., Goetz, S., Fatoyinbo, L., Hansen, M., Healey, S., Hofton, M., Hurtt, G., Kellner, J., Luthcke, S., et al., 2020. The global ecosystem dynamics investigation: high-resolution laser ranging of the earth?s forests and topography. Sci. Remote Sens. 1, 100002.

Dubayah, R., Hofton, M., Blair, J., Armston, J., Tang, H., and Luthcke, S., 2021. Gedi l2a elevation and height metrics data global footprint level v002. NASA EOSDIS Land Processes DAAC.

Dubayah, R., Tang, H., Armston, J., Luthcke, S., Hofton, M., Blair, J., 2021. Gedi l2b canopy cover and vertical profile metrics data global footprint level v002. NASA EOSDIS Land Processes DAAC.

Falkowski, M.J., Evans, J.S., Martinuzzi, S., Gessler, P.E., Hudak, A.T., 2009. Characterizing forest succession with lidar data: an evaluation for the inland northwest, USA. Remote Sens. Environ. 113 (5), 946–956.

Frelich, L.E., Reich, P.B., 2003. Perspectives on development of definitions and values related to old-growth forests. Environ. Rev. 11 (S1), S9–S22.

Gaines, G., Arndt, P., Croy, S., Devall, M., Greenberg, C., Hooks, S., Martin, B., Neal, S., Pierson, G., Wilson, D., 1997. Guidance for conserving and restoring old-growth forest communities on national forests in the southern region. Forestry Report R8-FR, 62.

Gillman, L.N., Wright, S.D., Cusens, J., McBride, P.D., Malhi, Y., Whittaker, R.J., 2015. Latitude, productivity and species richness. Glob. Ecol. Biogeogr. 24 (1), 107–117.

Gray, A.N., Brandeis, T.J., Shaw, J.D., McWilliams, W.H., Miles, P.D., et al., 2012. Forest inventory and analysis database of the united states of america (fia). Biodiversity Ecol. 4, 225–231.

Gray, A.N., Pelz, K., Hayward, G.D., Schuler, T., Salverson, W., Palmer, M., Schumacher, C., Woodall, C.W., 2023. Perspectives: The wicked problem of defining and inventorying mature and old-growth forests. For. Ecol. Manage. 546, 121350.

Hansen, A.J., Phillips, L.B., Dubayah, R., Goetz, S., Hofton, M., 2014. Regional-scale application of lidar: variation in forest canopy structure across the southeastern us. For. Ecol. Manage. 329, 214–226.

Helmer, E.H., Brown, S., Cohen, W., 2000. Mapping montane tropical forest successional stage and land use with multi-date landsat imagery. Int. J. Remote Sens. 21 (11), 2163–2183.

Hilbert, J., Wienszyk, A., 2007. Old-growth definitions and management: a literature review. J. Ecosyst. Manage.

Hirschmugl, M., Sobe, C., Di Filippo, A., Berger, V., Kirchmeir, H., Vandekerkhove, K., 2023. Review on the possibilities of mapping old-growth temperate forests by remote sensing in Europe. Environ. Model Assessment 1–25.

Hofton, M., Blair, J., Story, S., Yi, D., 2019. Algorithm Theoretical basis Document (atbd) for Gedi Transmit and Receive Waveform Processing for l1 and l2 Products. University of Maryland, College Park, MD, USA, p. 44.

Hurtt, G.C., Chini, L.P., Frolking, S., Betts, R., Feddema, J., Fischer, G., Fisk, J., Hibbard, K., Houghton, R., Janetos, A., et al., 2011. Harmonization of land-use scenarios for the period 1500–2100: 600 years of global gridded annual land-use transitions, wood harvest, and resulting secondary lands. Clim. Change 109, 117–161.

Kane, V.R., Bakker, J.D., McGaughey, R.J., Lutz, J.A., Gersonde, R.F., Franklin, J.F., 2010. Examining conifer canopy structural complexity across forest ages and elevations with lidar data. Can. J. For. Res. 40 (4), 774–787.

Keeton, W.S., Whitman, A.A., McGee, G.C., Goodale, C.L., 2011. Late-successional biomass development in northern hardwood-conifer forests of the northeastern united states. For. Sci. 57 (6), 489–505.

Kellogg, K., Hoffman, P., Standley, S., Shaffer, S., Rosen, P., Edelstein, W., Dunn, C., Baker, C., Barela, P., Shen, Y., Guerrero, A.M., Xaypraseuth, P., Sagi, V.R., Sreekantha, C.V., Harinath, N., Kumar, R., Bhan, R., Sarma, C.V.H.S., 2020. Nasa-isro synthetic aperture radar (nisar) mission. In 2020 IEEE Aerospace Conference, pages 1–21.

Körner, C., 2017. A matter of tree longevity. Science 355 (6321), 130–131.

Krieger, G., Moreira, A., Fiedler, H., Hajnsek, I., Werner, M., Younis, M., Zink, M., 2007. Tandem-x: a satellite formation for high-resolution sar interferometry. IEEE Trans. Geosci. Remote Sens. 45 (11), 3317–3341.

Ma, L., 2021. Advanced Modeling Using Land-Use History and Remote Sensing to Improve Projections of Terrestrial Carbon Dynamics. University of Maryland, College Park. PhD thesis.

Martin, M., Cerrejón, C., Valeria, O., 2021. Complementary airborne lidar and satellite indices are reliable predictors of disturbance-induced structural diversity in mixed old-growth forest landscapes. Remote Sens. Environ. 267, 112746.

May, P., McConville, K.S., Moisen, G.G., Bruening, J., Dubayah, R., 2023. A spatially varying model for small area estimates of biomass density across the contiguous united states. Remote Sens. Environ. 286, 113420.

Menlove, J., Healey, S.P., 2020. A comprehensive forest biomass dataset for the usa allows customized validation of remotely sensed biomass estimates. Remote Sens. 12 (24), 4141.

Moore, K.D., Nelson, M.P., 2023. The perilous and important art of definition: the case of the old-growth forest. Front. Ecol. Environ. 21 (6), 264–265.

Mosseler, A., Thompson, I., Pendrel, B., 2003. Overview of old-growth forests in canada from a science perspective. Environ. Rev. 11 (S1), S1–S7.

Omernik, J.M., Griffith, G.E., 2014. Ecoregions of the conterminous united states: evolution of a hierarchical spatial framework. Environ. Manage. 54 (6), 1249–1266.

Pederson, N., 2010. External characteristics of old trees in the eastern deciduous forest. Nat. Areas J. 30 (4), 396–407.

Pelz, K., Hayward, G., Gray, A., Berryman, E., Woodall, C., Nathanson, A., Morgan, N., 2023. Quantifying old-growth forest of united states forest service public lands. For. Ecol. Manage. 549, 121437.

Pesklevits, A., Duinker, P.N., Bush, P.G., 2011. Old-growth forests: anatomy of a wicked problem. Forests 2 (1), 343–356.

Pinto, N., Simard, M., Dubayah, R., 2012. Using insar coherence to map stand age in a boreal forest. Remote Sens. 5 (1), 42–56.

Piovesan, G., Biondi, F., 2021. On tree longevity. New Phytol. 231 (4), 1318–1337.

Pugh, S.A., Turner, J.A., Burrill, E.A., David, W., 2018. The Forest Inventory and Analysis Database: Population Estimation user Guide. USDA Forest Service, Washington DC, USA.

R Core Team, 2022. R: A Language and Environment for Statistical Computing. R Foundation for Statistical Computing, Vienna, Austria.

Spies, T.A., 2004. Ecological concepts and diversity of old-growth forests. J. For. 102 (3), 14–20.

Spracklen, B., Spracklen, D.V., 2021. Determination of structural characteristics of old-growth forest in ukraine using spaceborne lidar. Remote Sens. 13 (7), 1233.

Spracklen, B.D., Spracklen, D.V., 2019. Identifying european old-growth forests using remote sensing: a study in the ukrainian carpathians. Forests 10 (2), 127.

Stanke, H., Finley, A.O., Weed, A.S., Walters, B.F., Domke, G.M., 2020. rFIA: an r package for estimation of forest attributes with the us forest inventory and analysis database. Environ. Model. Software 127, 104664.

Stevens, J.T., Safford, H.D., North, M.P., Fried, J.S., Gray, A.N., Brown, P.M., Dolanc, C.R., Dobrowski, S.Z., Falk, D.A., Farris, C.A., et al., 2016. Average stand age from forest inventory plots does not describe historical fire regimes in ponderosa pine and mixed-conifer forests of western north america. PLoS One 11 (5), e0147688.

Tang, H., Armston, J., 2019. Algorithm Theoretical basis Document (atbd) for gedi l2b Footprint Canopy Cover and Vertical Profile Metrics. University of Maryland, College Park, MD, USA, p. 39.

Therneau, T., Atkinson, B., 2022. rpart: Recursive Partitioning and Regression Trees. R package version 4.1.19.

Therrell, M., Stahle, D., 1998. A predictive model to locate ancient forests in the cross timbers of osage county, Oklahoma. J. Biogeogr. 25 (5), 847–854.

Tyrrell, L.E., 1998. Information about old growth for selected forest type groups in the eastern United States, volume 197. US Department of Agriculture, Forest Service, North Central Forest.

Wickham, J., Stehman, S.V., Sorenson, D.G., Gass, L., Dewitz, J.A., 2021. Thematic accuracy assessment of the nlcd 2016 land cover for the conterminous united states. Remote Sens. Environ. 257, 112357.

Wirth, C., Messier, C., Bergeron, Y., Frank, D., Fankhänel, A., 2009. Old-Growth Forest Definitions: a Pragmatic View. Springer, Berlin Heidelberg, Berlin, Heidelberg.